Inorg. Chem. **2009**, *48*, 36−44

Inorganic Chemistry
Article

Molecular Construction, Characterization, and Photophysical Properties of Supramolecular Lanthanide−Calix[4]arene Covalently Bonded Hybrid Systems

Bing Yan,*,†,‡ Qian-Ming Wang,† and Dong-Jie Ma†

Department of Chemistry, Tongji University, Siping Road 1239 Shanghai 200092, China, and
State Key Laboratory of Rare Earth Materials Chemistry and Applications, Beijing 100871, China

Received March 19, 2008

Hydroxyl groups of the macrocyclic compound *p-tert*-butylcalix[4]arene have been converted into urethanesil (−NH(C═O)O−)-grafted bridges through a hydrogen transfer nucleophilic addition reaction. Subsequently, the modified macrocyclic derivative can coordinate to lanthanide ions (Tb, Eu) effectively and form a hybrid framework after the cohydrolysis and copolycondensation process through the triethoxysilane components. The above sol−gel-derived inorganic−organic supramolecular hybrids are analyzed under infrared spectroscopy, ultraviolet absorption, and luminescence spectroscopy for interpretation of their photophysical properties. Spectroscopic data point out that the modified calix[4]arene could sensitize diverse lanthanide ions to exhibit attractive green and red luminescence. It is noted that the triplet energy level of this particular macrocyclic bridged ligand is more suitable for the emissive energy level of Tb^{3+} ions than the Eu^{3+} ions. The luminescent lifetimes and quantum yields of europium hybrids are discussed, and the number of water molecules coordinated to Eu^{3+} is estimated.

Introduction

Luminescent materials, especially lanthanide phosphors, are applied in many devices of importance.[1] The interest in the photophysical properties of lanthanide complexes which act as optical centers in luminescent hybrid materials has grown considerably since Lehn[2] asserted that such complexes could be seen as light-harvesting supramolecular devices. Particularly, the design of efficient lanthanide complexes has acquired the attention of many research groups, focusing on the diverse classes of ligands, β-diketones, heterobiaryl ligands, etc. Our research group is focusing on the lanthanide ions (Eu, Tb, Sm, Dy) complexes with aromatic carboxylic acid components, bipyridyl, or their derivatives.[3−9] In recent decades, the sol−gel technology has been frequently employed in the synthesis of a significant number of unique attractive organic−inorganic hybrid materials with delicate control and a wide scope of practical applications.[10−13] Consequently, hybrid silicate materials derived from organo-bridged silsesquioxane precursors with molecular-scale homogeneity have now been considerably fabricated by this room temperature method. According to the chemical nature or different synergy between components, these hybrids can be categorized into two main classes. The first class concerns all systems where no covalent bond is present between organic and inorganic parts but only weak interactions such as hydrogen bonding, van der Waals force, or electrostatic forces.[12,13] These hybrids seem hard to prohibit the problem of quenching effect on luminescent centers due to the high vibration energy of the surrounding hydroxyl groups for generally they were prepared with conventional doping methods. Therefore, an alternative and very attractive possibility in regard to the complexation of lanthanide ions using

---

* To whom the correspondence should be addressed. E-mail: byan@tongji.edu.cn. Fax: +81-21-65982287. Phone: +81-21-65984663.

† Tongji University.

‡ State Key Laboratory of Rare Earth Materials Chemistry and Applications.

(1) Blasse, G. *J. Alloys Compd.* **1995**, *225*, 529.
(2) Lehn, J. M. *Angew. Chem., Int. Ed. Engl.* **1990**, *29*, 1304.
(3) Yan, B.; Song, Y. S. *J. Fluorescence* **2004**, *14*, 289.
(4) Song, Y. S.; Yan, B.; Chen, Z. X. *J. Solid State Chem.* **2004**, *177*, 3805.
(5) Yan, B.; Zhou, B. *J. Photochem. Photobiol. A. Chem* **2005**, *171*, 181.
(6) Wang, Q. M.; Yan, B.; Zhang, X. H. *J. Photochem. Photobiol. A. Chem.* **2005**, *174*, 119.
(7) Yan, B.; Xu, B. *J. Fluorescence* **2005**, *15*, 619.
(8) Yan, B.; Bai, Y. Y. *J. Fluorescence* **2005**, *15*, 605.
(9) Yan, B.; Wang, W. J. *J. Fluorescence* **2006**, *16*, 495.
(10) Leu, C. M.; Wu, Z. W.; Wei, K. H. *Chem. Mater.* **2002**, *14*, 3016.
(11) Nandi, M.; Conklin, J. A.; Salvati, L.; Sen, A. *Chem. Mater.* **1990**, *2*, 772.
(12) Tanner, P. A.; Yan, B.; Zhang, H. J. *J. Mater. Sci.* **2000**, *35*, 4325.
(13) Koslova, N. I.; Viana, B.; Sanchez, C. *J. Mater. Chem.* **1993**, *3*, 111.

10.1021/ic8004954 CCC: $40.75

ligands that are covalently fixed to the inorganic networks has emerged. To date, few studies in terms of covalently bonded hybrids with increasing chemical stability have appeared and the as-derived molecular-based materials exhibit monophasic appearance even at a "high concentration" of lanthanide complexes.[14−32] Some previous reports have been published on lanthanide−pyridinedicarboxylic acid complexes or their derivatives, and the feasibility of dicarboxylic acid systems has been firmly proved.[19] Zhang and co-workers started to modify 1,10-phenanthroline and dipyridine in order to prepare the determined molecular-level hybrid materials.[15,16] Our group recently put more emphasis on lanthanide coordination behavior and has now developed aromatic acid with modified amino, carboxyl, or hydroxyl groups[17,20,21,25,26] as "molecular bridges" which can not only develop chelating effects that can bind to lanthanide ions but also link to a silica host with an aminoalkoxysilane group.

In order to further optimize the light output and decrease the internal nonradiative decay processes, we first attempted macrocyclic molecules like calix[4]arenes to immobilize lanthanide ions. In 1978, Gutsche et al. synthesized a series of macrocyclic phenol formaldehyde condensates with the given name calixarenes and the molecular receptor activity is now their most significant property.[33] The successive search for new synthetic molecular receptors capable of guest−host relationships with metal ions and neutral molecules has triggered lots of novel structures during the past 20 years.[31] In regard to the attractive cavity in calixarene skeletons, we were motivated to modify the phenolic groups at the cup's lower rim of calix[4]arene with the electrophilic reagent 3-(triethoxysilyl)propyl isocyanate (TESPIC). The purpose of this work was to use calix[4]arene as molecular platforms to assemble groups of covalently bonded ligands capable of recognizing lanthanide ions.

In this report, totally different from previous studies on amino and carboxyl moiety groups, we attempt to modify active hydroxyl groups of calix[4]arene (Cali) by TESPIC-bearing trialkoxysilyl group as a functionalized organic ligand (abbreviated as Cali-Si) under sufficient basic environment. The excitation and luminescence spectra of the as-derived lanthanide covalently bonded hybrids are discussed in detail. In particular, the radiative lifetimes and quantum yields were measured.

Experimental Section

Chemicals and Procedures. 3-(Triethoxysilyl)propyl isocyanate was provided by Lancaster Synthesis Ltd. The solvents used were purified by common methods. Other starting reagents were used as received. Literature procedures were used to prepare calix[4]arene.[33]

A typical procedure for the preparation of Cali-Si was as follows: 1 mmol *p-tert*-butylcalix[4]arene was first dissolved in refluxing dehydrated tetrahydrofuran under stirring, and 4 mmol dehydrated K_2CO_3 (0.552 g) was added to the solution. Two hours later, 4 mmol (0.9 g) 3-(triethoxysilyl)propyl isocyanate was then put into the solution by drops for half an hour. The whole mixture was refluxing at 65 °C under argon for 8 h. After isolation and purification, a yellow oil Cali-Si was furnished. IR: −CONH− 1665 cm^{-1}, $-(CH_2)_3-$ 2917, 2969 cm^{-1}, Si−O 1086 cm^{-1}. Anal. Calcd. for $C_{74}H_{119}O_{16}N_3Si_3$: C 63.9, H 8.57, N 3.02; Found: C 62.8, H 8.31, N 3.01. ^1H NMR ($CDCl_3$) $C_{74}H_{119}O_{16}N_3Si_3$: δ 10.26 (1H, s), 8.60 (1H, s), 7.41 (1H, s), 7.18 (3H, t), 7.10 (1H, s), 7.06 (2H, d), 6.99 (1H, s), 6.89 (2H, d), 4.47 (8H, d), 3.83 (18H, m, $CH_2(OEt)$), 3.31 (6H, d), 1.87 (6H, s), 1.28 (36H, m, $C(CH_3)_3$), 1.22 (27H, m, $CH_3(OEt)$), 0.65 (6H, t).

The sol−gel-derived hybrid compounds containing lanthanide ions were prepared as follows: Cali-Si was dissolved in dimethylformamide (DMF) under stirring. A stoichiometric amount of $Ln(NO_3)_3 \cdot 6H_2O$ (Ln = Tb, Eu) was added to the solution. After 2 h, a corresponding amount of tetraethoxysilane (TEOS) was added in the reaction solution. Then one drop of diluted hydrochloric acid was put into it to promote hydrolysis. The molar ratio of $Ln(NO_3)_3 \cdot 6H_2O$/Cali-Si/TEOS/H_2O was 1:1:6:24. The mixture was agitated magnetically to achieve a single phase in a covered Teflon beaker, then it was aged at 80 °C until the onset of gelation which occurred within 5 days. Gels were collected as transparent monolithic bulks and ground as powder materials for the photophysical studies (see Figure 1).

Tb−calix[4]arene (or Eu−calix[4]arene) binary complex and Tb(Eu)-doped hybrid materials (named as Tb(Eu)-Cal/Si) were prepared simultaneously. The binary complex was synthesized according to the following procedure: *p-tert*-butylcalix[4]arene was dissolved in dehydrated dimethylformamide by dropping $Tb((NO_3)_3$ $(Eu((NO_3)_3)$ containing DMF solutions; the whole mixture was stirred under 70 °C for 3 h, and the precipitation was isolated and used without further purification. As for Tb (Eu)-doped hybrid materials, TEOS and water were stirred for 1 h and a drop of diluted hydrochloric acid was added to promote hydrolysis. The binary complex was then put into the solution. The molar ratio of Tb (Eu) binary complex/TEOS/H_2O was 1:10:40. The following treatment was the same as that for covalent hybrids.

The concentrations of Ln^{3+} ions in covalent hybrids were measured using the traditional complexometric titration method. The final hybrid samples were dissolved in nitric acid and then titrated with EDTA solution, using a buffer (pH 5.8) and xylenol-orange as indicator. The contents of Ln^{3+} are 10.11% for Tb^{3+} and 9.72% for Eu^{3+} that were in agreement with the stoichiometry $[Ln(Cali\text{-}Si)] \cdot 6SiO_2$ (Anal. Calcd: 10.17 for Tb; 9.77 for Eu) which verifies that each Cali-Si unit binds exactly one Ln ion for its large hindrance effect.

---

(14) Sanchez, C.; Lebeau, B. *Mater. Res. Soc. Bull.* **2001**, *26*, 377.
(15) Li, H. R.; Lin, J.; Zhang, H. J.; Fu, L. S. *Chem. Mater.* **2002**, *14*, 3651.
(16) Li, H. R.; Lin, J.; Zhang, H. J.; Fu, L. S. *Chem. Commun.* **2001**, 1212.
(17) Dong, D. W.; Jiang, S. C.; Men, Y. F.; Ji, X. L.; Jiang, B. Z. *Adv. Mater.* **2000**, *12*, 646.
(18) Franville, A. C.; Zambon, D.; Mahiou, R. *Chem. Mater.* **2000**, *12*, 428.
(19) Wang, Q. M.; Yan, B. *J. Mater. Chem.* **2004**, *14*, 2450.
(20) Wang, Q. M.; Yan, B. *Cryst. Growth Des.* **2005**, *5*, 497.
(21) Wang, Q. M.; Yan, B. *J. Mater. Res.* **2005**, *20*, 592.
(22) Wang, Q. M.; Yan, B. *J. Photochem. Photobiol. A: Chem.* **2006**, *175*, 159.
(23) Wang, Q. M.; Yan, B. *J. Photochem.Photobiol. A: Chem.* **2006**, *178*, 70.
(24) Wang, Q. M.; Yan, B. *J. Organomet. Chem.* **2006**, *691*, 540.
(25) Wang, Q. M.; Yan, B. *J. Organomet. Chem.* **2006**, *691*, 3567.
(26) Yan, B.; Ma, D. J. *J. Solid State Chem.* **2006**, *179*, 2059.
(27) Sui, Y. L.; Yan, B. *J. Photochem.Photobiol. A: Chem.* **2006**, *182*, 1.
(28) Yan, B.; Wang, F. F. *J. Organomet. Chem.* **2007**, *692*, 2395.
(29) Yan, B.; Qiao, X. F. *Photochem. Photobiol.* **2007**, *83*, 971.
(30) Lenaerts, P.; Driesen, K.; Deun, R. V.; Binnemans, K. *Chem. Mater.* **2005**, *17*, 2148.
(31) Carlos, L. D.; Ferreira, R. A. S.; Pereira, R. N.; Assuncao, M.; Bermudez, V. D. *J. Phys. Chem. B* **2004**, *108*, 14924.
(32) Carlos, L. D.; Ferreira, R. A. Sa.; Rainho, J. P.; Bermudez, V. de Zea. *Adv. Funct. Mater* **2002**, *12*, 819.
(33) Gutsche, C. D.; Muthurkrishnan, R. *J. Org. Chem.* **1978**, *43*, 4905.

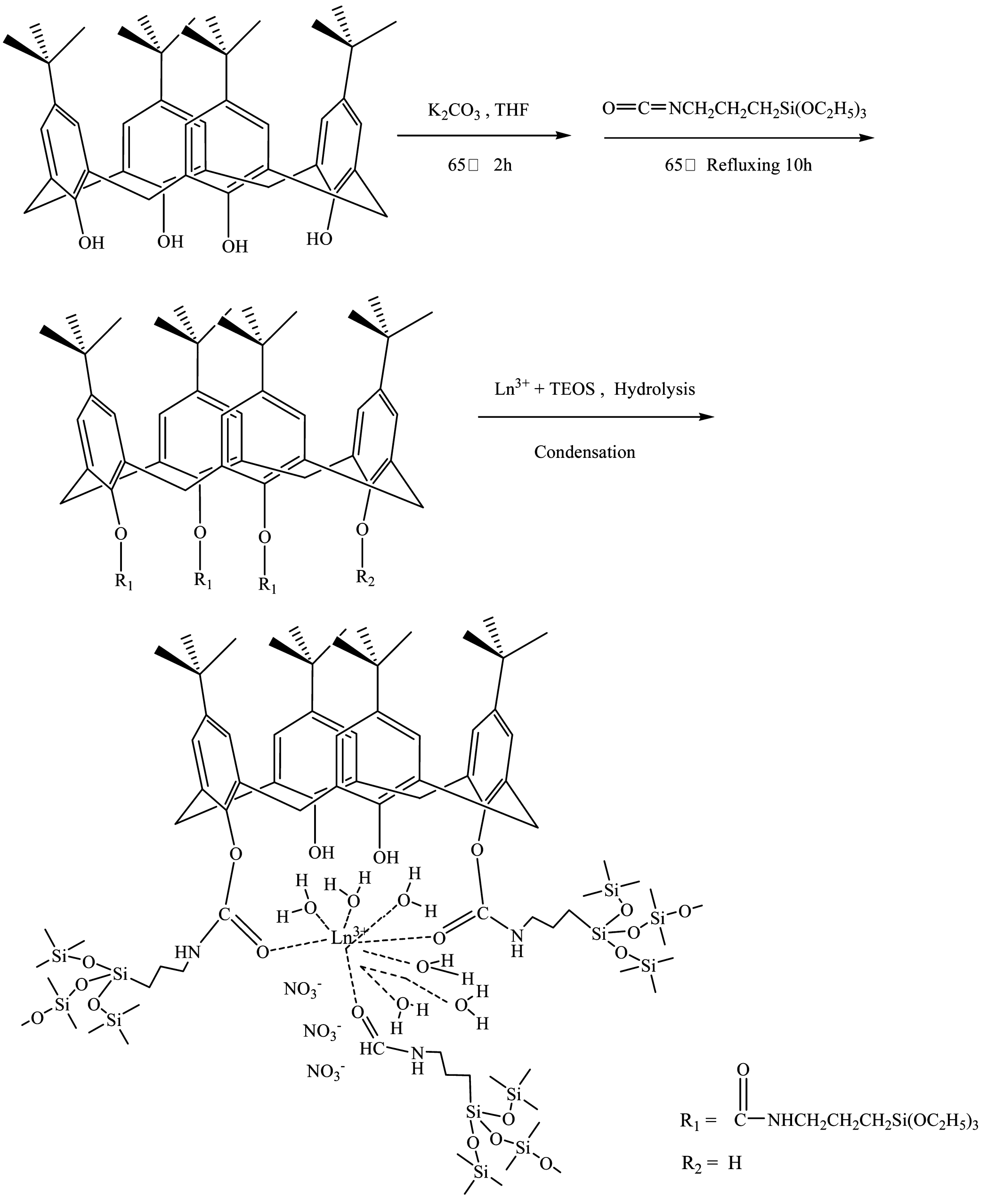

Figure 1. Predicted structure of terbium-centered covalently bonded hybrids.

Measurements. All measurements were completed under room temperature except for phosphorescence spectra (5×10^{-4} mol$\cdot$L^{-1} Acetone solution) which were measured at 77 K. ^{1}H NMR spectra were recorded in $CDCl_3$ on a Bruker AVANCE-500 spectrometer with tetramethylsilane (TMS) as internal reference. Elemental analyses (C, H, N) were determined with an Elementar Cario EL elemental analyzer. IR spectra were recorded with a Nicolet Nexus 912 AO446 spectrophotometer (KBr pellet), 4000−400 cm^{-1} region. Ultraviolet absorption spectra of these samples (5×10^{-4} mol$\cdot$L^{-1} acetone solution) were recorded with an Agilent 8453 spectrophotometer. Fluorescence excitation and emission spectra were obtained on a Perkin-Elmer LS-55 spectrophotometer. All the emission and excitation spectra were corrected, and the intensities were determined with integrated area. Luminescent lifetimes for hybrid materials were obtained with an Edinburgh Instruments FLS 920 phosphorimeter using a 450 W xenon lamp as excitation source (pulse width, 3 μs). The microstructures were checked by scanning electronic microscope (SEM, Philips XL-30).

Results and Discussion

3-(Triethoxysilyl)propyl isocyanate belongs to active silane cross-linking reagent molecules due to its positive carbon-containing isocyanate group, which can be expected to accept a Lewis base like unshared electron pair available for bonding. We have already achieved the hydrogen transfer addition reaction between TESPIC and $-NH_2$ derivatives.[20,21] In this particular type of mechanism, the more classical nucleophilic hydroxyl group attacks the partially positive carbonyl group of TESPIC. As shown in Figure 1, hydroxyl group derivatives, namely, *p*-*tert*-butylcalix[4]arenes can be modified by TESPIC to form the urethane (−OCO−NH−) linked functional bridge molecules Cali-Si. In order to clearly interpret the structure of resulting hybrids, we tried to modify all the four hydroxyl groups of *p*-*tert*-butylcalix[4]arene. The bridged ligands Cali-Si then play two

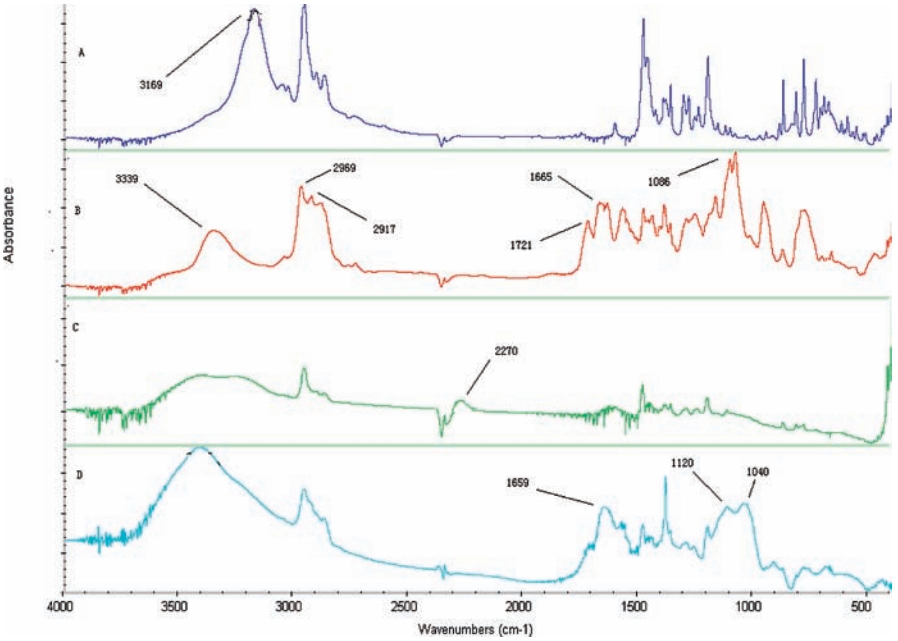

Figure 2. IR spectra of Cali (A), Cali-Si (B), unreacted calixarene (C), and Tb covalent hybrids (D).

roles: one is that they can coordinate to lanthanide ions through the oxygen atoms of their amide group; the other is that they can form covalently bonded Si−O network after the cohydrolysis and copolycondensation process with TEOS through their ethoxy groups (similar to the copolymerization of organic monomer with unsaturated bonds). Finally, the molecular-based hybrid materials can be assembled with strong chemical bonds (the coordination bond between Ln^{3+} and amide formations of bridging ligands and covalent bonds of Si−O network). These hybrid materials belong to a complicated huge molecular network.

The reaction model for the hybridization formula of TEOS and Cali-Si may be described as follows. The hybridization of TEOS and Cali-Si, accordingly, proceeds through a polycondensation reaction between the terminal silanol groups of Cali-Si and the OH groups of hydrolyzed TEOS. At the beginning of the reaction, the individual hydrolysis of Cali-Si and TEOS is predominant (step I). Step II is related to the polycondensation reactions between hydroxyl groups of both Cali-Si and TEOS (see Figure SI in Supporting Information). Meantime, the lone pairs of electrons owned by carbonyl groups within Cali-Si filled in the empty 4f orbits of lanthanide ions, thus forming new lanthanide complex molecules through donor and acceptor interactions. Silica gel exhibits weak emission at about 325 nm in the ultraviolet band which is attributed to be the charge transfer process between Si^{4+} atoms and O^{2-}.[35] According to the refs,35 and 36 we study the formation process of silica with luminescence lifetimes. During the cohydrolysis process of precursor sol composed with terbium ions, Cali-Si, TEOS, the luminescence lifetimes hardly change except for a slight improvement of luminescence intensities, which suggests that only intermolecular energy transfer process take place between Cali-Si and terbium ions and the terbium complex system with Cali-Si has not formed. After the polycondensation process of precursor and formation, we further found that the luminescence lifetimes of gel enhance more than the corresponding sol, which indicates that the terbium coordination systems with Cali-Si formed after the in situ sol−gel process.

Figure 2 displays the IR spectra of Cali (A), Cali-Si (B), unreacted calixarene with TESPIC (C) and Tb covalent hybrids (D). From Figure 2A,B, we can notice that the −OH vibration at 3169 cm^{-1} (A) was shifted to a broadband located at 3339 cm^{-1} (B) which was overlapped by the absorption of −NH− groups. In Figure 2B, no characteristic band at approximately 2270 cm^{-1} ascribed to the vibration of R-NCO terminal group was observed (in Figure 2C, the peak still exists), showing that the grafting reaction was rather complete. In addition, the sharp bands in Figure 3B located at 2969 and 2917 cm^{-1} together with the absorption of $-CH_2-$ groups in calixarene were attributed to the stretching vibration of CH_2 moieties on the coupling agent. According to L. D. Carlos,[37] the grafted "amide I" mode has hypersensitive response to the specific environment and the influence of hydrogen bond among N−H−O atoms. The vibration of C═O in Figure 2B was identified as two distinct components centered at 1721 and 1665 cm^{-1}, respectively. The 1721 cm^{-1} peak shows that hydrogen-bonded C═O groups were largely connected to each other while the band at 1665 cm^{-1} gives a common vibration of CONH groups with highly ordered hydrogen-bonded aggregation. Furthermore, the strong bands at approximately 1086 cm^{-1} correspond to the vibration absorption of $Si-OC_2H_5$ bonds. It is worth mentioning that we overestimated the electrophilic reactivity of TESPIC initially and when adopting it to attack

---

(34) Atwood, J. L.; Barbour, L. J.; Hardie, M. J.; Raston, C. L. *Coord. Chem. Rev.* **2002**, *222*, 3.

(35) Gracia, J.; Mondragon, M. A.; Tellez, C. *Mater. Chem. Phys.* **2002**, *41*, 15.

(36) Elsayed, M. A.; Bhaumik, M. L. *J. Chem. Phys.* **1963**, *39*, 2391.

(37) Goncalves, M. C.; de Zea Bermudez, V.; Sa. Ferreira, R. A.; Carlos, L. D.; Ostroviskii, D.; Rocha, J. *Chem. Mater.* **2004**, *16*, 2530.

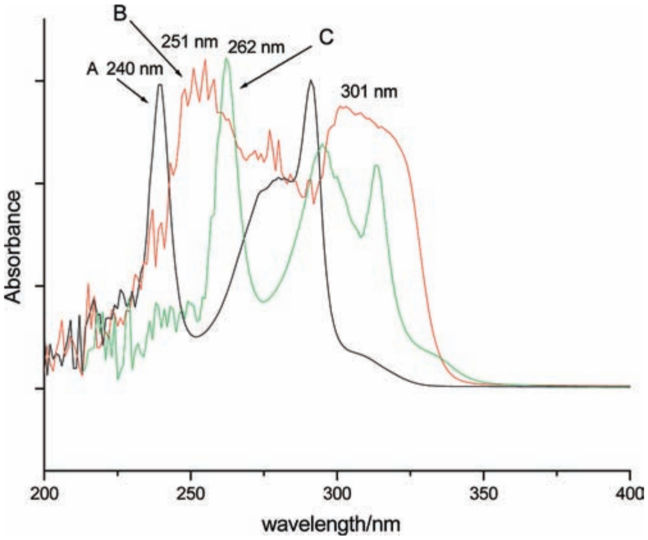

Figure 3. Ultraviolet absorption spectra of (A) Cali, (B) Cali-Si, and (C) Tb-Cali-Si (5×10^{-4} mol·L^{-1} acetone solution).

the hydroxyl groups of Cali, but the IR results for the crude product given by Figure 2C substantiated that the grafting reaction was not successful until the stoichiometric amount of potassium carbonate base was added to increase the nucleophilic capability of oxygen anions. It was observed from Figure 2D that the vibration of C=O at 1721 cm^{-1} disappeared and absorption of CONH groups at 1665 cm^{-1} blue-shifted to 1659 cm^{-1} after forming complexes with Tb^{3+}. Additionally, the broadband from 1120 to 1040 cm^{-1} was attributed to the formation of matrices SiO$_2$ backbone.

Ultraviolet spectroscopy measurements (Figure 3) designate the presence of unsaturated systems, and Figure 3A for Cali shows characteristic transition wavelengths of aromatic ligands at about 240 and 291 nm. As regards Figure 3B (Cali-Si), corresponding red shift (240 → 251, 291 → 301 nm) substantiates that a more extensive $\pi-\pi^*$ conjugating system was formed due to the grafting reaction of TESPIC. As for B and C (Tb-centered covalent hybrids), further red shift (251 → 262 nm) and splitting of the peak at 301 nm firmly give the evidence of the complexes formation between Tb^{3+} and Cali-Si ligands. The overlap between the excitation spectra of Tb-centered hybrids (A) and the absorption of Cali-Si(B) are also shown in Figure 4. This particular observation clearly proves the typical sensitization of terbium ions by Cali-Si ligands, called "antenna effect", and thus confirms the modified calixarenes, especially through grafted carbonyl subunits, were self-assembled and bonded around the lanthanide core.

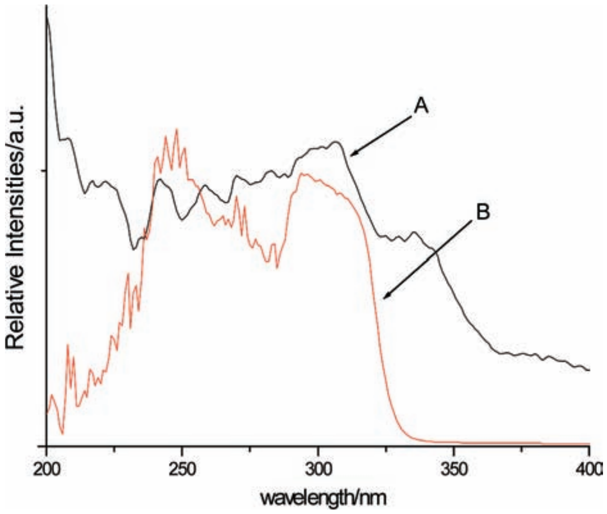

Figure 4. Excitation spectra of Tb-centered hybrids (solid powders) (A) and the absorption of Cali-Si (5×10^{-4} mol·L^{-1} acetone solution) (B).

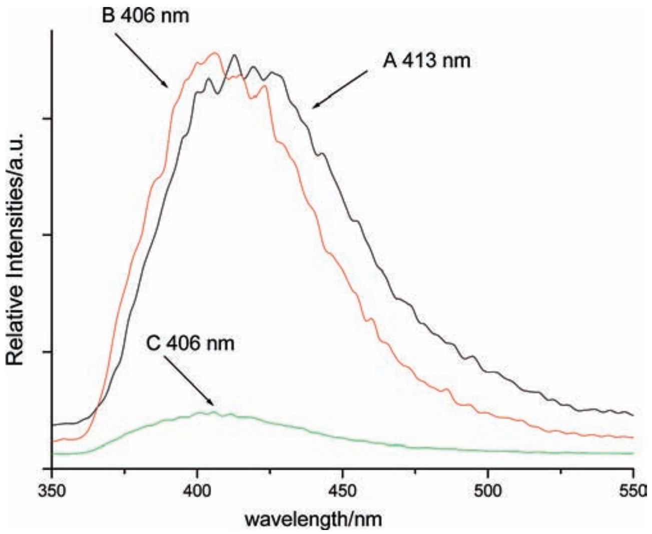

Figure 5. Phosphorescence spectra of Cali (A), Cali-Si (B), and Tb-Cali-Si (C) (5×10^{-4} mol·L^{-1} acetone solution).

The phosphorescence spectra of Cali (Figure 5A) and Cali-Si (Figure 5B) show a 7 nm blue shift (A → B, 413 → 406 nm). In terms of Figure 6, B and C (Tb-centered covalent hybrids), there is no change between the two curves with only the difference of their intensities for the same Cali-Si ligand, showing that Cali-Si effectively sensitizes and transfers part of its energy to the terbium ions when the energy level of the triplet state belonging to ligands lies higher than the emission state of the Tb^{3+}. According to Sato's result,[38] the intramolecular energy migration efficiency from organic ligands to the central Ln^{3+} is the most important factor determining the luminescence properties of lanthanide complexes.[39] The intramolecular energy transfer efficiency is established mainly on two energy transfer processes.[40,41] One is from the lowest triplet state energy of organic ligands to the resonant energy level by Dexter's resonant exchange interaction theory:[42]

$$k_{\mathrm{ET}} = K(2\pi Z^2/R)\int F_{\mathrm{d}}(E)E_{\mathrm{a}}(E)\,\mathrm{d}E\,\exp(-2R_{\mathrm{da}}/L) \qquad (1)$$

The other is the inverse energy transition by thermal deactivation mechanism:[43]

---

(38) Sato, S.; Wada, M. *Bull. Chem. Soc. Jpn.* **1970**, *43*, 1955.
(39) Wu, S. L.; Wu, Y. L.; Yang, Y. S. *J. Alloys Compd.* **1994**, *180*, 399.
(40) Zhang, H. J.; Yan, B.; Wang, S. B.; Ni, J. Z. *J. Photochem. Photobiol. A.* **1997**, *109*, 223.
(41) Yan, B.; Zhang, H. J.; Wang, S. B.; Ni, J. Z. *J. Photochem. Photobiol. A.* **1998**, *116*, 209.
(42) Dexter, D. L. *J. Chem. Phys.* **1953**, *21*, 836.
(43) Brown, T. D.; Shepherd, T. M. *J. Chem. Soc., Dalton Trans.* **1973**, 336.

$$k(T) = A\exp(-\Delta E/RT) \qquad (2)$$

Here k_{ET} is the rate constant of the intramolecular energy transfer. $2\pi Z^2/R$ is a constant relative to the specific mutual distance between the central Ln^{3+} ion and its coordinated atoms (O or N). $F_d(E)$ and $E_a(E)$ are the experimental luminescence spectrum of energy donor (ligands) and the experimental absorption spectrum of energy acceptor (Ln^{3+}), respectively, so both of them represent the overlap spectrum of Ln^{3+} cations. R_{da} is the intramolecular distance between donor atoms and acceptor atoms, and L is the van der Waals radius. Both R_{da} and L may be considered to be constant in intramolecular transfer processes, so k_{ET} is proportional to the overlap of $F_d(E)$ and $E_a(E)$. With the decrease of the energy difference between the triplet state of conjugated carboxylic acid and Ln^{3+} excited levels, the overlap of $F_d(E)$ and $E_a(E)$ is increased. So from eq 1, it can be concluded that the more the overlap between the luminescence spectrum of organic ligands and the excited-state energy levels of Ln^{3+} ions, the more the intramolecular energy rate constant k_{ET}. On the other hand, the activation energy ΔE in eq 2 is equal to the energy difference $\Delta E(\text{Tr-Ln}^{3+})$, while from the formula, the inverse energy transfer rate constant $k(T)$ increased with decreasing $\Delta E(\text{Tr-Ln}^{3+})$. As discussed above, there should exist an optimal energy difference between the triplet state position of Cali-Si and the excited energy level of Ln^{3+} ions, the larger for eq 1 and the smaller for eq 2. $\Delta E(\text{Tr-Ln}^{3+})$ will decrease the luminescence properties of lanthanide complexes. In consequence, the energy level differences between the lowest triplet state energy of Cali-Si (24630 cm^{-1}) and the resonant emitting levels of Tb^{3+} (20 500 cm^{-1}) or Eu^{3+} (17 265 cm^{-1}) are 4130 and 7365 cm^{-1}, respectively, suggesting that the specific energy transfer mechanism is more favorable for Tb^{3+} than for Eu^{3+} ions. The following emission spectra obtained from Tb and Eu hybrids further demonstrate our predicted conclusion.

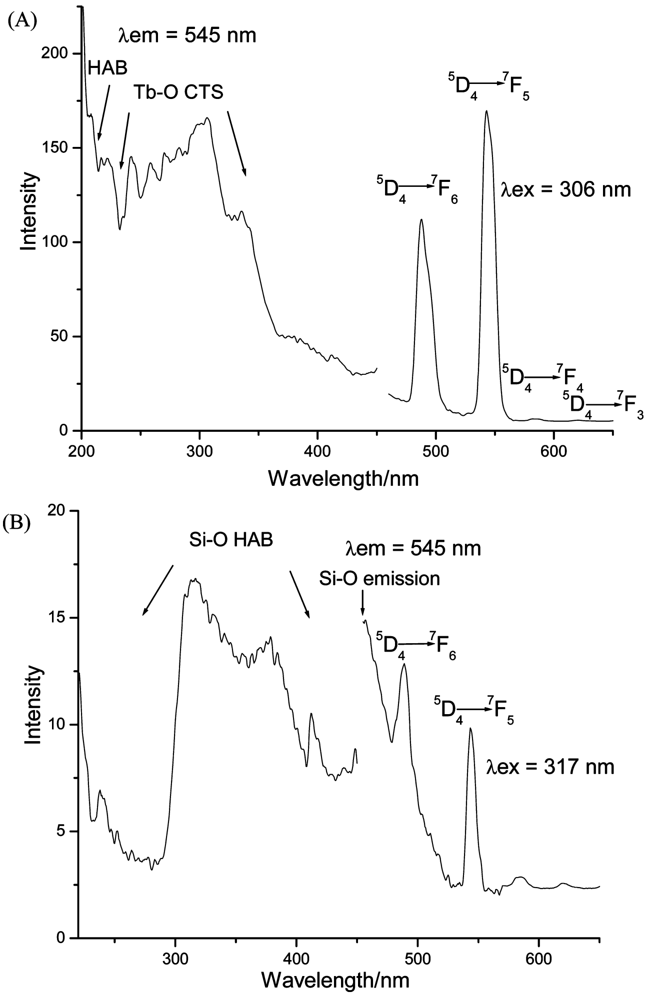

Figure 6. Excitation and emission spectra of Tb covalently bonded hybrids (Tb-Cal-Si, A) and Tb-doped hybrids (Tb-Cal/Si, B) (solid powders).

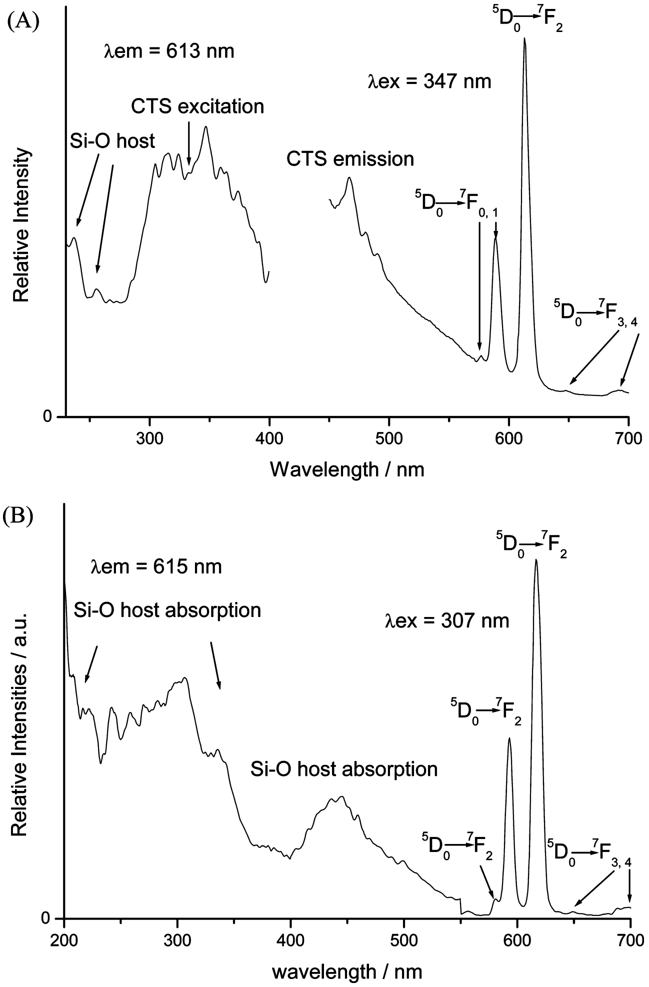

Figure 7. Excitation and emission spectra of Eu covalently bonded hybrids (Eu-Cal-Si, A) and Tb-doped hybrids (Eu-Cal/Si, B) (solid powders).

The photoluminescence spectra of Tb and Eu covalently bonded hybrid materials and Tb- and Eu-doped materials are shown in Figures 6 and 7. The excitation spectrum in Figure 6A for covalently bonded Tb hybrids is monitored at 545 nm and no obvious f−f transitions are detected because they are quite weak and forbidden. The observed broadband at the range of 280−400 nm with peak of 306 nm is ascribed to Tb−O charge transfer state (CTS) absorption transitions. Besides, some weak peaks below 250 nm belong to the host absorption (HAB). So the emission spectra were measured under excitation wavelength of 306 nm. The intense narrow peaks observed in the luminescence spectrum are transitions from the $^5D_4$ excited state to the different J levels of the ground state ^7F_J ($J = 6, 5, 4, 3$), showing the organic ligands

Cali-Si act as an efficient antenna for terbium ions. Figure 6B displays the spectra of common Tb-doped materials whose excitation spectrum consists of a broadband from 290 to 420 nm. This band should be ascribed to the Si−O network absorption and not to CTS of Tb−O because with the low doped concentration it is hard to form the strong CTS. It can be observed that a high baseline exists in front of the $^5D_4 \rightarrow {}^7F_6$ transition in the emission spectrum. This may be induced by the influence of emission transition of Si−O network owing to Cali-Si ligands and silicate hosts. Furthermore, its luminescence intensity was largely decreased compared with covalently bonded hybrids (Figure 6B). This firmly indicates that grafted carbonyl groups in benzene groups combined in Cali-Si ligands effectively coordinate to central ions in contrast to weak metal recognition function provided by substituted −OH groups in calix[4]arenes.

With regard to Figure 7A, for the luminescent spectrum of covalently bonded europium hybrids, a broad excitation band ranged in 280−400 nm centered at 350 nm in the long-wavelength UV range, corresponding to the charge transfer state (CTS) of Eu−O. The strong CTS absorption is favorable for the efficient energy transfer to Eu^{3+}, and the effective luminescence of Eu^{3+} can be expected. Besides, a weak absorption band in the range of short-wavelength ultraviolet region 200−250 nm occurs, corresponding to the host absorption of Si−O network. No f−f transitions could be observed in the spectra (they are too weak). $^5D_0 \rightarrow {}^7F_2$ transition that is hypersensitive to the environment appears dominantly in the spectra, showing that europium ion occupies in the lattice a site with slight deviations from inversion symmetry. Because covalent hybrids are amorphous, the emission transitions are broad accordingly and the electric dipole transition $^5D_0 \rightarrow {}^7F_2$ may include magnetic dipole transition $^5D_0 \rightarrow {}^7F_1$. The luminescence behaviors of all of the materials have been investigated by direct excitation of the ligands (347 nm). The maxima of these bands are at around 590 and 613 nm associated with $^5D_0 \rightarrow {}^7F_1$ and $^5D_0 \rightarrow {}^7F_2$ transitions, respectively. A prominent feature that may be noted in these spectra is the very high intensity of the $^5D_0 \rightarrow {}^7F_2$ transition. $^5D_0 \rightarrow {}^7F_1$ transition is magnetic−dipolar transition and insensitive to their local structure environment while $^5D_0 \rightarrow {}^7F_2$ transition is electric−dipolar transition and sensitive to the coordination environment of the Eu^{3+} ion. When the interactions of the rare-earth complex with its local chemical environment are stronger, the complex becomes more nonsymmetrical and the intensity of the electric−dipolar transitions becomes more intense. Figure 7B shows the luminescent spectra of europium doped hybrids, which exhibits a similar feature to the covalently bonded one except that its intensity is weaker. The excitation spectrum consists of broad absorption bands for the Si−O network. Five apparent emission peaks can be observed at 581, 593, 616, 649, 698 nm, respectively, corresponding to the Eu^{3+}'s transitions $^5D_0 \rightarrow {}^7F_J$ ($J = 0, 1, 2, 3, 4$).

Table 1. Luminescent Data for Lanthanide−Calix[4]arene Supramolecular Colvalently Bonded Hybrids

lanthanide hybrids	Eu-Cali-Si	Eu-Cali/Si	Tb-Cali-Si	Tb-Cali/Si
emission bands	577, 589, 614, 647, 694	580, 592, 616, 649, 698	489, 545, 588, 622	
A_{00} (s^{-1})	2.3	5.4		
A_{01} (s^{-1})	50	50		
A_{02} (s^{-1})	128	103		
A_{03} (s^{-1})	0.9	2.2		
A_{04} (s^{-1})	1.0	3.7		
τ (ms)^a	0.18	0.13	0.49	0.42
A_{rad} (s^{-1})	181	165		
$\tau_{exp}{}^{-1}$ (s^{-1})	5556	7693		
A_{nrad} (s^{-1})	5375	7528		
η (%)	3.26	2.14		
n_W	5.6			

^{a} For $^5D_0 \rightarrow {}^7F_2$ transition of Eu^{3+}, for $^5D_4 \rightarrow {}^7F_5$ transition of Tb^{3+}.

The typical decay curve of the hybrid materials all can be described as a single exponential ($\mathrm{Ln}(S(t)/S_0) = -k_1t = -t/\tau$) (see Figure SII in Supporting Information). This indicates that all lanthanide ions occupy the same average coordination environment. The resulting lifetimes of Tb, Eu, Sm, and Pr hybrids were given in Table 1. Further, we selectively determined the emission quantum efficiencies of the $^5D_0$ excited state of europium ion for Eu^{3+} covalently bonded hybrids and doped hybrids on the basis of the emission spectra and lifetimes of the $^5D_0$ emitting level; the detailed luminescent data are shown in Table 1. The quantum efficiency of the luminescence step, η, expresses how well the radiative processes (characterized by rate constant A_r) compete with nonradiative processes (overall rate constant A_{nr}).[44−52]

$$\eta = A_r/(A_r + A_{nr}) \tag{3}$$

Nonradiative processes influence the experimental luminescence lifetime by the equation:[44−52]

$$\tau_{exp} = (A_r + A_{nr})^{-1} \tag{4}$$

So quantum efficiency can be calculated from radiative transition rate constant and experimental luminescence lifetime from the following equation:[44−52]

$$\eta = A_r\tau_{exp} \tag{5}$$

where A_r can be obtained by summing over the radiative rates A_{0J} for each $^5D_0 \rightarrow {}^7F_J$ transition of Eu^{3+}.[44−52]

$$A_r = \sum A_{0J} = A_{00} + A_{01} + A_{02} + A_{03} + A_{04} \tag{6}$$

The branching ratio for the $^5D_0 \rightarrow {}^7F_{5,6}$ transitions can be neglected as they both are not detected experimentally, and

---

(44) Werts, M. H. V.; Jukes, R. T. F.; Verhoeven, J. W. *Phys. Chem. Chem. Phys.* **2002**, *4*, 1542.

(45) Peng, C. Y.; Zhang, H. J.; Yu, J. B.; Meng, Q. G.; Fu, L. S.; Li, H. R.; Sun, L. N.; Guo, X. M. *J. Phys. Chem. B* **2005**, *109*, 15278.

(46) Carlos, L. D.; Messaddeq, Y.; Brito, H. F.; Ferreira, R. A. S.; Bermudez, V. D.; Ribeiro, S. J. L. *Adv. Mater.* **2000**, *12*, 594.

(47) Ferreira, R. A. S.; Carlos, L. D.; Goncalves, R. R.; Ribeiro, S. J. L.; Bermudez, V. D. *Chem. Mater.* **2001**, *13*, 2991.

(48) Soares-Santos, P. C. R.; Nogueira, H. I. S.; Felix, V.; Drew, M. G. B.; Ferreira, R. A. S.; Carlos, L. D.; Trindade, T. *Chem. Mater.* **2003**, *15*, 100.

(49) Teotonio, E. E. S.; Espinola, J. G. P.; Brito, H. F.; Malta, O. L.; Oliveria, S. F.; de Foria, D. L. A.; Izumi, C. M. S. *Polyhedron* **2002**, *21*, 1837.

(50) Ribeiro, S. J. L.; Dahmouche, K.; Ribeiro, C. A.; Santilli, C. V.; Pulcinelli, S. H. J. *J. Sol-Gel Sci. Technol.* **1998**, *13*, 427.

(51) Malta, O. L.; Couto dos Santos, M. A.; Thompson, L. C.; Ito, N. K. *J. Lumin.* **1996**, *69*, 77.

(52) Malta, O. L.; Brito, H. F.; Menezes, J. F. S.; Goncalves e Silva, F. R.; Alves, S.; Farias, F. S.; Andrade, A. V. M. *J. Lumin.* **1997**, *75*, 255.

whose influence can be ignored in the depopulation of the ${}^5D_0$ excited state.[46−48] Since ${}^5D_0 \rightarrow {}^7F_1$ belongs to the isolated magnetic dipole transition, it is practically independent of the chemical environments around the Eu^{3+} ion, and thus can be considered as an internal reference for the whole spectrum; the experimental coefficients of spontaneous emission, A_{0J}, can be calculated according to the relation[49]

$$A_{0J} = A_{01}(I_{0J}/I_{01})(\upsilon_{01}/\upsilon_{0J}) \tag{7}$$

Here A_{0J} is the experimental coefficient of spontaneous emission, and A_{01} is Einstein's coefficient of spontaneous emission between the ${}^5D_0$ and ${}^7F_1$ energy levels. In vacuum, A_{01} has a value of 14.65 s^{-1}; when an average index of refraction n equal to 1.506 was considered, the value of A_{01} can be determined to be 50 s^{-1} approximately ($A_{01} = n^3 A_{01(\mathrm{vacuum})}$).[45,50] I is the emission intensity and can be taken as the integrated intensity of the ${}^5D_0 \rightarrow {}^7F_J$ emission bands.[51,52] υ_{0J} refers to the energy barrier and can be determined from the emission bands of Eu^{3+}'s ${}^5D_0 \rightarrow {}^7F_J$ emission transitions. Here, the emission intensity, I, taken as integrated intensity S of the ${}^5D_0 \rightarrow {}^7F_{0-4}$ emission curves.[45] On the basis of the above discussion, the quantum efficiencies can be estimated and the covalently bonded europium hybrid material (3.26%) is higher than that of europium-doped one (2.14%), which corresponds to the similar rule to their lifetimes. The covalently bonded hybrids can decrease the nonradiative transition compared to the doped hybrids. Certainly, we also can see that both the two europium hybrid are not higher than 10%, suggesting the energy match for Eu^{3+} is not suitable and the energy transfer to Eu^{3+} is not effective.

Besides, the 1:1 molar ratio of Ln^{3+} and Cali-Si can be predicted with content of Ln in covalently bonded hybrid materials. In order to study the coordination environment surround lanthanide ions especially the influence caused by vibrations of water molecules, according to Horrocks' previous research,[53,54] it is therefore expected that the probable number of coordinated water molecules (n_w) can be calculated by the following equation:

$$n_w = 1.05(A_{\mathrm{exp}} - A_{\mathrm{rad}}) \tag{8}$$

in which A_{rad} and A_{nrad} are radiative and nonradiative probabilities, respectively. τ_{exp} is decay time of Eu-containing covalent hybrids. A_{rad} can be described as the ratio of relative intensities of ${}^5D_0 \rightarrow {}^7F_J$ ($J = 6, 5, 4, 3$) transitions. The values of A_{rad}, A_{nrad}, and n_w were calculated through the above three equations and are reported in Table 1. Based on the results, the coordination number of water molecules (Eu containing hybrid materials) can be estimated to be 6. The coordinated water molecules produce severe vibration of the hydroxyl group, resulting in the large nonradiative transition and decreasing the luminescent efficiency.

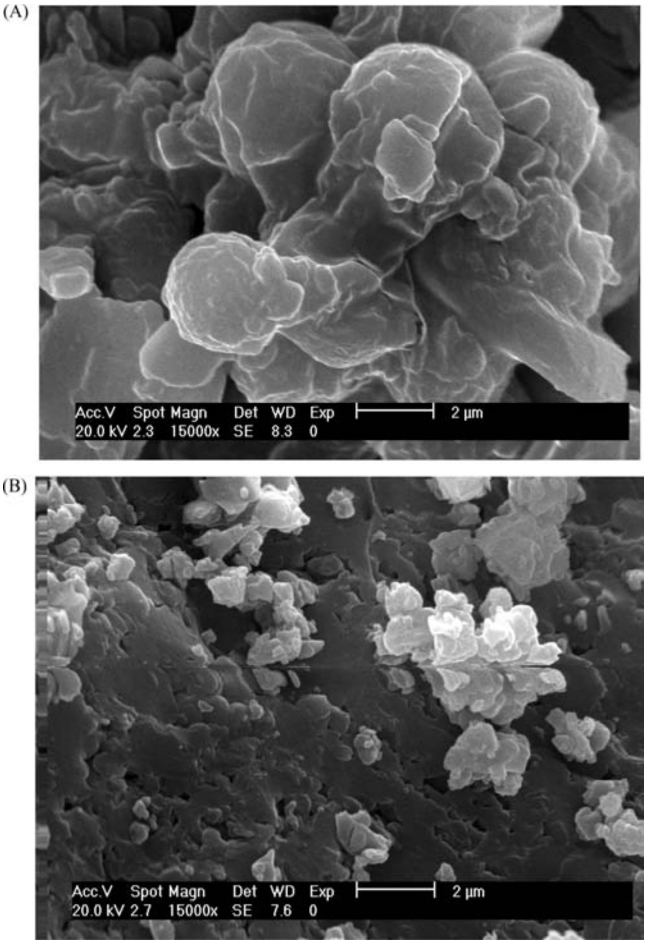

Figure 8. Scanning electron images for Tb covalently bonded hybrids (Tb-Cal-Si, A) and Tb-doped hybrids (Tb-Cal/Si, B).

Figure 8 compares the SEM pictures of covalently bonded hybrids (A) and the doped ones (B). The former appears to be very homogeneous and uniform, which may be caused primarily by Cali-Si ligands acting as a double functional bridge between inorganic matrices and luminescent cations. Moreover, quite a few spheroids (diameter approximately 2−3 μm) emerged in the fracture surface and we predicted that both the coupling agent TESPIC and the cuplike macrocyclic calix[4]arene triggered the formation of such attractive morphology, whereas in general calix[4]arene-doped silicate materials exhibited obvious phase separation because the organic moieties were simply dispersed into the surface of host lattice without powerful chemical bond linkages. This is in agreement with the luminescent behaviors of lifetimes and quantum efficiencies for covalently bonded hybrids and doped hybrids.

Conclusions

The coordination behavior between urethanesil groups and metal ions and the fine recognition ability of calix[4]arene allowed us to design two (Tb, Eu) novel molecular-level hybrid materials and study their photophysical properties. Calix[4]arene was modified with 3-(triethoxysilyl)propyl isocyanate) (TESPIC) through a hydrogen transfer nucleophilic addition reaction and acted as a cross-linking intermediate which plays a double role. In view of coordination chemistry, it can coordinate lanthanide ions through carbonyl groups; on the other side, the hydrolysis and polycondensation reactions among triethoxysilyl groups of Cali-Si and

---

(53) Horrocks, W. De W.; Sudnick, D. R. *J. Am. Chem. Soc.* **1979**, *101*, 334.

(54) Horrocks, W. De W.; Sudnick, D. R. *Acc. Chem. Res.* **1981**, *14*, 384.

TEOS lead to the formation of Si−O−Si network structures. Consequently, the corresponding green, red, and blue luminescent supramolecular hybrid systems with chemical bond were attained. Of all the photoluminescent hybrids, Tb covalently bonded hybrid material shows the strongest luminescence and for the suitable energy match between Cal-Si and Tb^{3+}. The covalently bonded hybrid materials present longer lifetimes than the doped hybrid ones; especially, the luminescent quantum efficiency of covalently europium hybrids is higher than that of the doped europium one. The existence of coordination water molecules to lanthanide ions produces severe nonradiative energy loss to decrease the luminescent properties.

Acknowledgment. This work was supported by the National Natural Science Foundation of China (20671072).

Supporting Information Available: Figures SI and SII showing polycondensation and complexation processes of Cali-Si and Tb^{3+} ions, and typical decay curve of the Tb covalently bonded hybrid material. This material is available free of charge via the Internet at http://pubs.acs.org.

IC8004954